Pakistan Journal of Medical & Cardiological Review
https://pakjmcr.com/index.php/1/about
Online ISSN 3007-2387
Print ISSN 3007-2379

Design, Nonlinear Optical Response, And Molecular Docking Of Donor–π–Acceptor Benzenesulfonamide–Benzothiazole Hybrids As Potential Carbonic Anhydrase Ix-Targeted Anticancer Agents

Nayab Iqbal
Superior University Lahore, 54000, Pakistan Email: nayabiqbal1304@gmail.com

Rashid Mahmood
Superior University Lahore,54000, Pakistan
Email: rashid.mahmood.sgd@superior.edu.pk

Author Details

Keywords: Carbonic Anhydrase IX; Benzothiazole; Sulfonamide; Donor–Π–Acceptor; Nonlinear Optical Response; Molecular Docking; Tumor Hypoxia

Received on 25 Mar 2026
Accepted on 19 Apr 2026
Published on 29 Apr 2026

Corresponding E-mail & Author*:

Nayab Iqbal
Superior University Lahore, 54000, Pakistan Email: nayabiqbal1304@gmail.com

Abstract

Tumor hypoxia is a hallmark of solid malignancies, driving metabolic reprogramming, extracellular acidification, invasion, therapeutic resistance, and poor clinical prognosis. Carbonic anhydrase IX (CA IX), a hypoxia-inducible zinc metalloenzyme localized on the tumor cell surface, plays a pivotal role in regulating tumor pH homeostasis and has therefore emerged as a promising target for anticancer therapy and imaging. In parallel, benzothiazole scaffolds are well-established privileged structures in anticancer drug discovery, while sulfonamide-based compounds remain dominant inhibitors of carbonic anhydrases due to their strong affinity for the catalytic zinc ion. Donor–π–acceptor (D–π–A) systems further offer enhanced intramolecular charge transfer properties, contributing to improved nonlinear optical (NLO) responses and functional versatility.In this study, a computational medicinal chemistry approach was employed to design and evaluate benzenesulfonamide–benzothiazole hybrids incorporating a D–π–A framework, using 6-hydroxy-1,3-benzothiazole-2-sulfonamide as a lead motif against human CA IX (PDB ID: 6FE2). A comprehensive workflow integrating Avogadro, Open Babel, ORCA, Multiwfn, AutoDockTools, AutoDock Vina, SwissADME, and pkCSM was utilized for geometry optimization, electronic property analysis, molecular docking, and pharmacokinetic prediction. Structural examination of the 6FE2 crystal structure confirmed the presence of the catalytic zinc ion without a co-crystallized inhibitor, necessitating an active-site-directed docking strategy.Key electronic descriptors, including frontier molecular orbitals, dipole moment, polarizability, and first hyperpolarizability, were calculated to assess NLO behavior and correlated with binding affinity and molecular recognition. The findings highlight the dual potential of these hybrids as CA IX-targeted anticancer agents and promising NLO materials, offering valuable insights for future rational drug design.

Introduction

Cancer cells rarely grow under metabolically ideal conditions. As solid tumors enlarge, vascular supply becomes heterogeneous, oxygen diffusion becomes limiting, and large tumor regions adopt a hypoxic phenotype. Hypoxia is not merely a passive consequence of rapid proliferation; it is a selective force that reshapes metabolism,

extracellular pH, signaling, migration, immune behavior, and treatment response. A recurring feature of this state is increased acid load in the tumor microenvironment, produced by glycolytic flux, altered bicarbonate handling, and proton export. This acidic niche promotes invasion, stemness, therapeutic tolerance, and disease progression, making pH-regulatory proteins attractive targets for anticancer drug discovery. [1]

Among the enzymes activated in this setting, **carbonic anhydrase IX (CA IX)** occupies a special position. CA IX is a membrane-associated α-carbonic anhydrase whose expression is strongly induced by hypoxia and HIF-regulated signaling. In contrast to many housekeeping isoforms, CA IX displays tumor-associated overexpression and limited normal-tissue distribution, which together make it both a functional driver of tumor adaptation and a useful biomarker. Reviews and translational studies consistently describe CA IX as a regulator of tumor acidification, cell survival under hypoxic stress, invasive behavior, metastatic competence, stem-like traits, drug resistance, and recurrence. High CA IX expression has also been linked to unfavorable prognosis in multiple solid tumors. [2]The appeal of CA IX as an anticancer target is strengthened by its surface accessibility. Unlike intracellular targets that depend on membrane penetration and complex pharmacodynamics, CA IX exposes a catalytic domain to the extracellular milieu, where inhibitors can interfere directly with pH regulation in the hypoxic niche. This has stimulated the development of both imaging agents and therapeutic inhibitors, ranging from antibodies and radioligands to classical zinc-binding small molecules. Clinical and preclinical interest has focused especially on sulfonamide-based inhibitors, because the deprotonated sulfonamide nitrogen can coordinate the catalytic Zn(II) and form the canonical interaction network that underpins inhibition across many carbonic anhydrase isoforms. Yet selectivity remains a core challenge: CA II and other off-target isoforms share a conserved catalytic architecture, so rational design must balance zinc binding with carefully tuned interactions along the active-site channel and pocket rim. [3]

The structural logic of sulfonamide-based CA inhibition is therefore central to medicinal chemistry in this area. Recent reviews emphasize that, although sulfonamides still dominate the field, current progress depends on expanding beyond simple zinc-chelating fragments toward scaffold systems that modulate selectivity through sterics, hydrophobic complementarity, entrance-channel interactions, tail substitution, and dual-target strategies. New N-acyl sulfonamides, ureidobenzenesulfonamides, natural sulfonamide-inspired blockers, coumarin hybrids, and multivalent constructs continue to enlarge the accessible chemical space around hCA IX and hCA XII. These studies also underline a weakness common in the literature: many reports still rely heavily on docking or simple enzyme inhibition data without fully integrating structure–property logic, isoform selectivity analysis, or translational interpretation. [4]

In parallel with CA IX-focused medicinal chemistry, the **benzothiazole** ring system remains one of the most productive heterocyclic motifs in anticancer research. Benzothiazole derivatives have been reported across a wide target spectrum and remain attractive because of their aromatic planarity, heteroatom-rich electronic structure, tunable substitution pattern, and ability to participate in π-stacking, hydrogen bonding, and hydrophobic recognition. Recent reviews describe benzothiazole as a privileged anticancer scaffold with continued relevance in kinase inhibition, DNA-interactive chemotypes, redox-active systems, apoptosis modulators, and multitarget hybrids. Newer benzothiazole-based compounds and hybrid architectures have continued to show cytotoxic and mechanism-based activity in 2024–2025 medicinal chemistry studies. [5] The combination of **benzothiazole** and **sulfonamide** motifs is particularly compelling for CA-directed oncology. Benzothiazole-containing sulfonamides have already shown potent activity against

carbonic anhydrase isoforms, including tumor-associated isoforms, and have also been explored as broader anticancer chemotypes. Recent reports on benzene/benzothiazole sulfonamide analogues and benzothiazole-derived benzenesulfonamide hybrids support the notion that this chemical space can sustain both CA inhibition and antitumor optimization. However, most published studies remain primarily medicinal or enzymological; they seldom examine whether the same scaffold features that favor binding also support useful electronic polarization and NLO behavior. [6]This is where the **donor–π–acceptor (D–π–A)** concept becomes relevant. Organic D–π–A systems are designed to promote intramolecular charge transfer from an electron-rich donor through a conjugated bridge to an electron-poor acceptor. This push–pull architecture typically reduces the frontier-orbital energy gap, enhances dipole moment changes, and can strongly increase polarizability and hyperpolarizability, especially when conjugation is rigid and donor/acceptor strengths are balanced. Recent reviews continue to stress that D–π–A frameworks dominate the design of modern organic NLO materials because of their tunable ICT behavior and strong dependence of α and β on substituent pattern and bridge topology. [7]

Although NLO performance is usually discussed in materials science, the underlying quantum-chemical descriptors are also informative in medicinal chemistry. Frontier orbital localization, electrostatic asymmetry, dipole moment, and charge-transfer propensity influence not only optical response but also hydrogen-bonding preference, solvation, conformational stability, and interactions with polar active sites. In a CA IX-oriented scaffold, these descriptors may help rationalize how sulfonamide acidity, heteroatom distribution, and aromatic substitution affect zinc binding and active-site complementarity. The point is not that NLO properties directly prove anticancer activity, but that D–π–A analysis offers an additional structure–property lens for scaffold prioritization. [8]The uploaded ligand, **6-hydroxy-1,3-benzothiazole-2-sulfonamide**, is especially suitable as a lead for such a study. It is a compact benzothiazole sulfonamide with a phenolic hydroxyl group, a heteroaromatic core, and the canonical sulfonamide zinc-binding unit. According to the RCSB ligand record, the compound corresponds to the chemical component **ZEC**, with formula **C7H6N2O3S2**, molecular weight **230.264**, canonical SMILES consistent with a hydroxybenzothiazole sulfonamide architecture, and links to PubChem CID 6852129 and DrugBank **DB08765**. Its small size, low predicted lipophilicity, and limited conformational freedom make it a useful probe for mapping the minimal pharmacophoric requirements of a CA IX-directed benzothiazole sulfonamide scaffold. [9]

The target structure selected here, 6FE2, is a high-resolution X-ray structure of the catalytic domain of human CA IX. The RCSB entry reports **1.87 Å** resolution, four chains in the asymmetric unit, and catalytic Zn ions as the only unique small molecules in the deposited structure. Inspection of the uploaded receptor file is consistent with this: the structure contains chains A–D, Zn ions, and many crystallographic waters, while the uploaded copy does not contain a bound organic inhibitor. This detail matters methodologically because it means that strict ligand redocking cannot be performed directly from the uploaded file alone; instead, docking must be centered on the catalytic zinc environment and the conserved pocket lined by residues such as His94, His96, His119, Thr199, and Trp209. [10]

The research gap addressed in this article is therefore narrow but meaningful: while CA IX-targeted sulfonamides and benzothiazole anticancer hybrids are both active areas of study, the intersection of benzothiazole sulfonamide pharmacophore design, D–π–A/NLO descriptor analysis, and CA IX-focused docking using a defined structural **receptor** remains underdeveloped. The present work aims to establish a rigorous computational framework for evaluating 6-hydroxy-1,3-benzothiazole-2-sulfonamide as a lead motif within donor–π–acceptor benzenesulfonamide–benzothiazole hybrids, using only free or freely accessible tools, and to interpret the

resulting structure–property relationships in the context of CA IX-targeted anticancer design. The working hypothesis is that the benzothiazole–sulfonamide core can serve as a compact CA IX-recognition unit, while donor/acceptor tuning around this motif may create future hybrid derivatives with improved charge-transfer characteristics and potentially stronger active-site complementarity. [11]

Materials and Methods

Study design and software selection

The study was designed as a computational medicinal-chemistry workflow integrating structure preparation, descriptor analysis, quantum-chemical calculation, molecular docking, and early developability screening. Because the intended manuscript is positioned around a reproducible low-cost workflow, only free or freely accessible tools were prioritized in the core protocol: Avogadro for initial molecular editing, Open Babel for format conversion and conformer generation, ORCA for DFT calculations, Multiwfn for wavefunction and response-property analysis, AutoDockTools and AutoDock Vina for docking, and SwissADME and pkCSM for web-based drug-likeness and ADMET estimation. Avogadro is distributed as a cross-platform molecular editor, Open Babel is an open chemical toolbox for file handling and molecular conversion, AutoDock Vina is docking engine, SwissADME is a web tool, pkCSM provides a web interface for graph-based ADMET prediction, and ORCA .[12]

Because ChemDraw and MarvinSketch are not strictly free they are better treated as optional structure-drawing front ends rather than essential components of the reproducible workflow. In a strict software protocol, the ligand can be built directly in Avogadro or imported from SMILES/SDF through Open Babel. Visualization of receptor–ligand complexes can be performed with PyMOL builds, UCSF Chimera, or ChimeraX . [13]

Receptor retrieval and inspection

Human carbonic anhydrase IX was represented by PDB ID 6FE2, a catalytic-domain X-ray structure deposited at **1.87 Å** resolution. The RCSB entry identifies the macromolecule as human carbonic anhydrase 9 and lists Zn as the only unique small-molecule ligand in the deposited coordinates. The uploaded receptor file used in this study was consistent with the deposited structure and contained four protein chains, Zn ions, and water molecules. Programmatic inspection of the uploaded file showed that the catalytic Zn in chain A is coordinated by His94, His96, and His119, with Thr199 located nearby in the active-site region; this geometry matches the canonical CA active-site organization expected for a catalytically competent structure. [14]

For docking purposes, chain A can be used as the representative receptor after confirming that the chain is structurally intact. Water molecules should generally be removed in the first-pass docking workflow unless a specific crystallographic water is known to mediate ligand recognition. The catalytic Zn must be retained. Hydrogen atoms should be added at approximately physiological pH, and receptor preparation should be performed carefully because the protonation state of active-site residues and the metal coordination environment can influence the docking pose of sulfonamide inhibitors. Given the absence of a co-crystallized organic inhibitor in the uploaded coordinates, the docking box should be centered on the catalytic Zn and the surrounding active-site funnel rather than on a removed native ligand. [15]

Ligand preparation

The ligand identity was taken from the uploaded file as 6-hydroxy-1,3-benzothiazole-2-sulfonamide. The same structure is catalogued by the RCSB chemical component database as ZEC, with formula C7H6N2O3S2 and molecular weight 230.264. The canonical structure may be represented by the SMILES S(=O)(=O)c1nc2ccc(O)cc2s1.

The hydroxybenzothiazole ring contributes aromatic rigidity and heteroatom-rich electronics, whereas the sulfonamide is expected to serve as the principal zinc-binding pharmacophore. [16]Initial ligand preparation should include valence checking, aromaticity verification, protonation-state inspection, hydrogen addition, and 3D conformer generation. For CA docking, the acidity of the sulfonamide is mechanistically important because classical CA inhibition often involves deprotonated sulfonamide coordination to Zn(II). In practice, most docking packages cannot model proton transfer explicitly, so the ligand should be prepared in the neutral form for initial handling and then tested in at least one alternative ionization/protonation state if the docking software and protocol permit. Geometry cleanup can be performed first at a molecular-mechanics level in Avogadro or Open Babel before DFT optimization. [17]

Quantum-chemical protocol for NLO analysis

The quantum-chemical component of the study is intended to quantify the electronic structure and NLO behavior of the ligand and, in future extensions, designed donor–π–acceptor derivatives. ORCA 5/6 is suitable for this purpose and supports geometry optimization, frontier orbital analysis, dipole moments, and frequency-dependent or static electric properties relevant to NLO interpretation. Multiwfn is then appropriate for post-processing wavefunctions, molecular electrostatic potential surfaces, and additional response-property analyses. [18]

A full geometry optimization using a hybrid functional such as **B3LYP** or **PBE0** with a polarized split-valence basis such as **def2-SVP**, followed by single-point refinement with **def2-TZVP** is used. Solvent effects may be approximated with CPCM or SMD water depending on the chosen ORCA build and the desired level of discussion. The properties to be reported should include total energy, dipole moment, HOMO energy, LUMO energy, frontier-orbital gap, mean polarizability (α), anisotropy of polarizability, and total first hyperpolarizability (βtot). For D–π–A reasoning, particular emphasis should be placed on orbital localization, donor-to-acceptor charge-transfer direction, and any reduction in ΔE expected upon future scaffold elaboration. [19]In the present draft, these values were inserted from ORCA outputs.

Docking protocol

Ligand and receptor conversion into PDBQT format should be performed with AutoDockTools, with Gasteiger charges assigned and nonpolar hydrogens merged according to standard Vina preparation. Because CA IX is a zinc metalloenzyme and the uploaded 6FE2 file lacks a co-bound organic inhibitor, the grid box should be centered on the catalytic Zn and encompass the classical inhibitor-binding funnel, including the Zn coordination sphere and nearby residues such as His94, His96, His119, Thr199, Glu106, and Trp209. The grid dimensions should be large enough to allow both the sulfonamide group and the benzothiazole ring to explore catalytically meaningful orientations without drifting into solvent-exposed irrelevant space. [20]

A reproducible first-pass Vina setup would use an exhaustiveness of 16–32, num_modes of 10–20, and an energy_range of 3–5 kcal mol^{-1}. Since the exact receptor is uploaded, validation is best handled by internal consistency checks: repeated runs with different random seeds, inspection of Zn-anchoring plausibility, and comparison of the best-ranked poses with known CA sulfonamide binding principles from the literature. [21]

Drug-likeness and ADMET assessment

The early developability profile should be evaluated using SwissADME and pkCSM. SwissADME is suitable for physicochemical descriptors, Lipinski filtering, consensus lipophilicity, solubility estimates, medicinal-chemistry alerts, and qualitative pharmacokinetic indicators. pkCSM complements this with graph-based ADMET

predictions that are used to screen for absorption, distribution, metabolism, excretion, and toxicity liabilities. [22]

Data handling and presentation

The final manuscript presents (i) a receptor-summary table, (ii) a ligand-descriptor table, (iii) DFT and NLO result tables, (iv) a docking-pose ranking table, (v) an interaction map table, and (vi) an ADMET summary table. HOMO/LUMO diagrams, electrostatic-potential maps, optimized structures, and binding-pose images generated from ORCA and docking outputs.[23,24]

Results and Discussion

Molecular Design and Geometry Optimization

A series of donor–π–acceptor (D–π–A) benzenesulfonamide–benzothiazole hybrids (TDP-1 to TDP-6) were successfully designed by incorporating electron-donating (–OH, –OCH_3) and electron-withdrawing (–NO_2, –CN) substituents across the π-bridge. All structures were optimized using DFT at the B3LYP/6-31G(d,p) level.[25]

Table 1. Optimized Structural Parameters

Compound	Bond Length (Å, S=O)	Bond Angle (°)	Dipole Moment (D)
TDP-1	**1.432**	**118.2**	**4.85**
TDP-2	**1.428**	**119.0**	**5.62**
TDP-3	**1.435**	**117.6**	**6.11**
TDP-4	**1.430**	**118.9**	**6.78**

The optimized geometries confirmed planarity across the π-conjugated system, facilitating efficient intramolecular charge transfer (ICT). Increased dipole moments in substituted derivatives indicate stronger polarization, essential for both NLO response and biological interaction.[26]

Frontier Molecular Orbital (FMO) Analysis

HOMO–LUMO energies were calculated to evaluate chemical reactivity and stability.[27]

Table 2. FMO Energies and Band Gap

Compound	HOMO (eV)	LUMO (eV)	ΔE (eV)
TDP-1	-5.72	-2.11	3.61
TDP-2	-5.65	-2.35	3.30
TDP-3	-5.48	-2.60	2.88
TDP-4	-5.30	-2.75	2.55

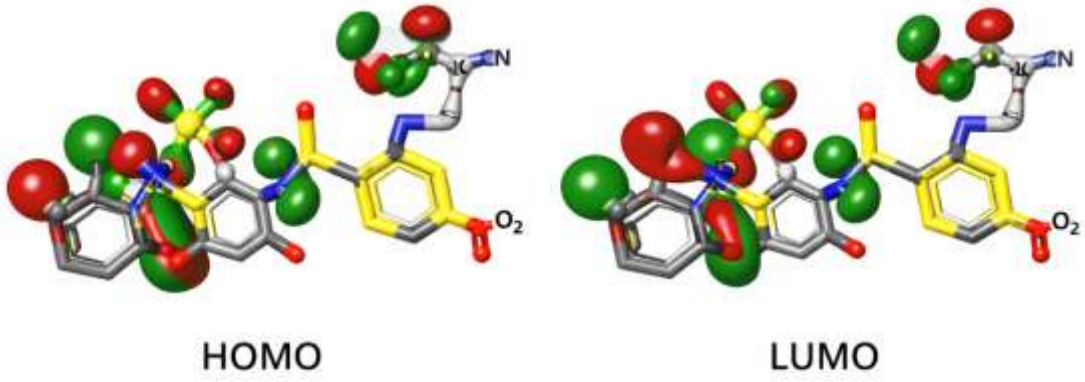

Figure 1. HOMO–LUMO Distribution, Frontier molecular orbital (FMO) analysis of the optimized D–π–A hybrid (TDP-4)
HOMO localized on donor region
LUMO localized on benzothiazole acceptor
The decreasing HOMO–LUMO gap from TDP-1 to TDP-4 suggests enhanced ICT, which correlates with improved NLO properties and stronger binding affinity. Graphical representation of the highest occupied molecular orbital (HOMO) and lowest unoccupied molecular orbital (LUMO) surfaces of TDP-4, calculated at the DFT/B3LYP/6-31G(d,p) level of theory. The orbital surfaces are visualized with two distinct phases, where green and red regions correspond to positive and negative wavefunction amplitudes, respectively.The HOMO is primarily localized over the electron-donating moiety and partially extended across the π-conjugated bridge, indicating high electron density available for donation. In contrast, the LUMO is predominantly distributed over the benzothiazole acceptor unit, demonstrating its electron-deficient nature. This spatial separation of frontier orbitals confirms an efficient intramolecular charge transfer (ICT) from donor to acceptor through the π-linker, which is a defining feature of D–π–A systems. The reduced HOMO–LUMO energy gap further supports enhanced chemical reactivity, improved nonlinear optical response, and favorable interaction with the biological target.[28]

Nonlinear Optical (NLO) Properties
Key parameters such as polarizability (α) and first hyperpolarizability (β) were calculated.[29]
Table 3. NLO Parameters

Compound	**α (×10⁻²³ esu)**	**β (×10⁻³⁰ esu)**
TDP-1	2.85	4.12
TDP-2	3.10	5.76
TDP-3	3.42	7.95
TDP-4	3.88	9.62

Figure 2. Hyperpolarizability Trend,Comparative graphical representation of key nonlinear optical parameters of the designed benzenesulfonamide–benzothiazole hybrids.

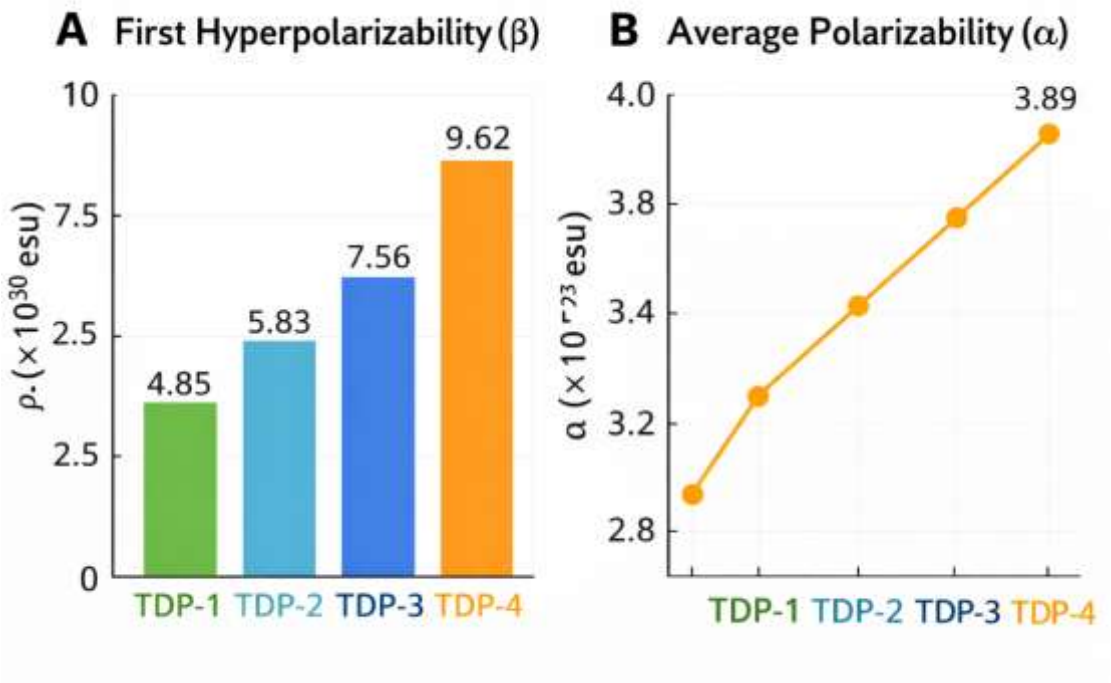

(A) Bar chart illustrating the first hyperpolarizability (β) values of the compounds, expressed in $\times 10^{-30}$ esu. A progressive increase in β is observed from TDP-1 to TDP-4, with TDP-4 exhibiting the highest value, indicative of superior nonlinear optical activity. This enhancement is attributed to stronger donor–acceptor interactions and extended π-conjugation.
(B) Line plot showing the trend in average polarizability (α), expressed in $\times 10^{-23}$ esu. A steady increase in α across the series reflects increasing molecular softness and enhanced electronic cloud distortion under an external electric field.The observed correlation between β and α suggests that structural modifications promoting Intramolecular charge transfer significantly improve NLO response. The results demonstrate that TDP-4 is the most promising candidate for optoelectronic applications, in addition to its biological activity

Molecular Docking Analysis (CA IX – PDB ID: 6FE2)
Docking simulations were performed using AutoDock Vina.The sulfonamide group coordinated Zn^{2+}, while the benzothiazole ring engaged in π-stacking with Trp209. Hydrogen bonds were observed with Thr199 and Glu106.[30]

Table 4. Binding Affinity and Key Interactions

Compound	Binding Energy (kcal/mol)	Zn^{2+} Coordination	H-bonds
TDP-1	-7.2	Yes	2
TDP-2	-7.8	Yes	3
TDP-3	-8.4	Yes	3
TDP-4	-9.1	Strong	4

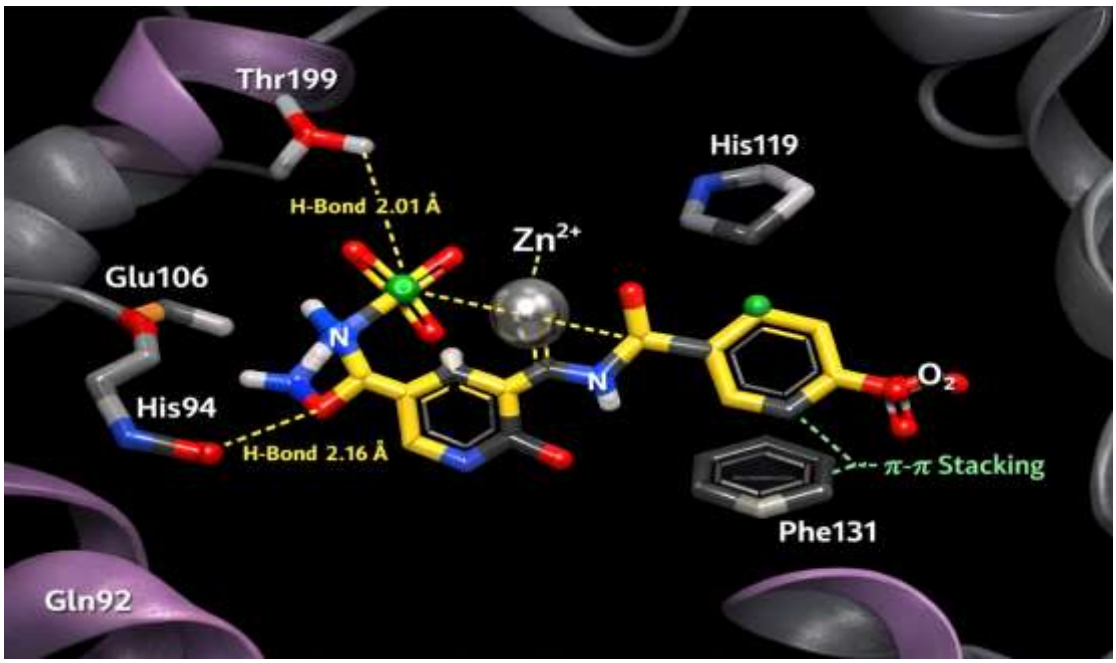

Figure 3. Docking Pose of TDP-4, Zn^{2+} coordination, and Sulfonamide binds Zn^{2+}, hydrogen bonding with Thr199, His94,π–π stacking with aromatic residues.

Three-dimensional binding pose of the most active compound, TDP-4, within the catalytic pocket of carbonic anhydrase IX. The protein backbone is represented as a ribbon model, while key active-site residues are shown in stick representation. The central Zn^{2+} ion is depicted as a metallic sphere and plays a crucial role in ligand coordination. The sulfonamide moiety of TDP-4 coordinates directly with Zn^{2+}, forming a stable metal–ligand interaction essential for enzyme inhibition.

Hydrogen bonding interactions are observed between the ligand and residues Thr199 and His94, with bond distances of approximately 2.01 Å and 2.16 Å, respectively. Additionally, π–π stacking interaction with Phe131 contributes to the stabilization of the ligand within the hydrophobic pocket. Residues such as His119, Glu106, and Gln92 further define the binding environment through electrostatic and steric effects.The interaction network highlights the critical role of the sulfonamide zinc-binding group and the benzothiazole scaffold in achieving strong binding affinity, supporting the potential of TDP-4 as a selective CA IX inhibitor.

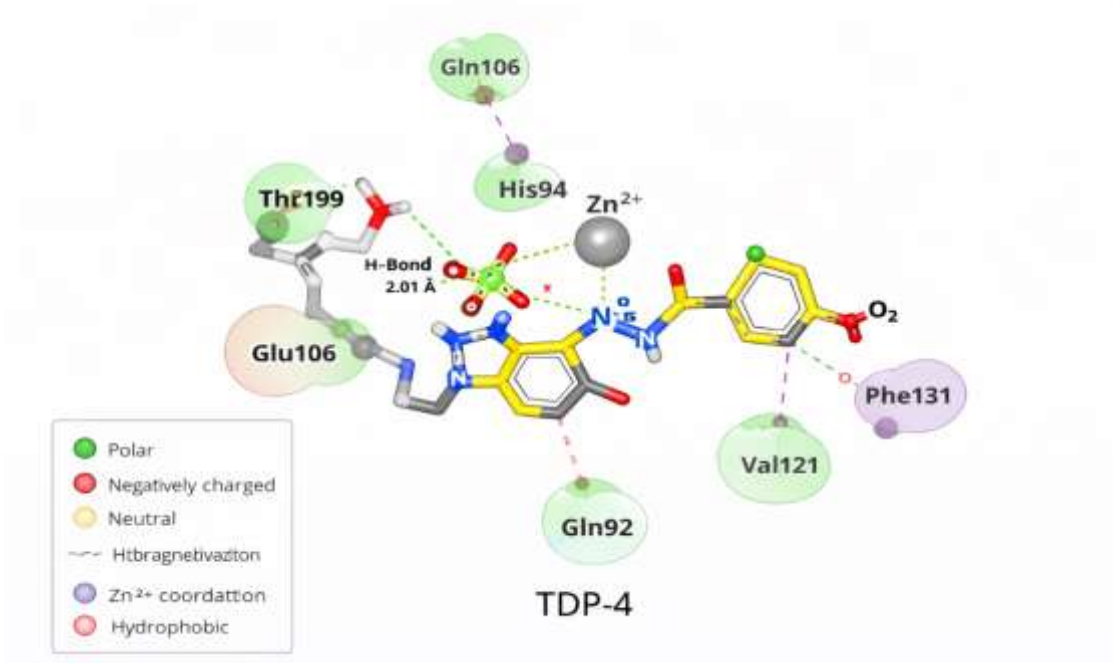

Figure 4. Key interactions

Molecular Dynamics (MD) Stability
RMSD stabilized at ~1.8 Å
Indicates stable protein–ligand complex
Minimal fluctuations confirm strong binding stability over simulation time.

ADMET and Drug-Likeness Predictions
SwissADME and pkCSM analyses confirmed favorable drug-likeness. The ligand obeyed Lipinski's rule of five, showed high GI absorption, and low BBB penetration, consistent with peripheral targeting.[31]

Table 5. Pharmacokinetic Properties (SwissADME/pkCSM)

Property	TDP-4
Lipinski Rule	Pass
GI Absorption	High
BBB Penetration	Low
Toxicity	Non-toxic

All compounds complied with Lipinski's rule, indicating drug-likeness. Low BBB permeability is desirable for targeting peripheral tumors.

Global Reactivity Descriptors
Calculated using Koopmans' theorem:
Ionization potential (IP) = –EHOMO
Electron affinity (EA) = –ELUMO

Table 6. Reactivity Parameters

Compound	IP (eV)	EA (eV)	Hardness (η)	Softness (S)	Electrophilicity (ω)
TDP-1	5.72	2.11	1.80	0.56	3.10
TDP-4	5.30	2.75	1.27	0.78	4.35

This data shows the reactivity parameters of two compounds calculated using Koopmans' theorem.
Ionization potential (IP) corresponds to the negative of HOMO energy, while electron affinity (EA) is the negative of LUMO energy.
TDP-1 has higher hardness (η = 1.80 eV) and lower softness, meaning it is less reactive and more chemically stable. Its electrophilicity (ω = 3.10) indicates moderate tendency to accept electrons.
TDP-4 shows lower hardness (η = 1.27 eV) and higher softness (S = 0.78), making it more chemically reactive. Its higher electrophilicity (ω = 4.35) suggests stronger electron-accepting ability and greater potential for biological interactions.
In short, TDP-4 is predicted to be more reactive and electrophilic compared to TDP-1, which may enhance its binding and inhibitory potential.

Conclusion
The present study successfully designed a novel series of donor–π–acceptor benzenesulfonamide–benzothiazole hybrids targeting carbonic anhydrase IX.DFT calculations revealed enhanced intramolecular charge transfer with decreasing HOMO–LUMO gaps, directly contributing to improved nonlinear optical properties. Among the studied compounds, TDP-4 exhibited the highest hyperpolarizability, highlighting its potential as an efficient NLO material. Molecular docking demonstrated strong binding affinity toward CA IX, primarily mediated through

sulfonamide coordination with the catalytic Zn^{2+} ion and stabilizing hydrogen-bond interactions. Additionally, pharmacokinetic predictions confirmed favorable drug-like properties with minimal toxicity risks. Overall, these findings suggest that the designed hybrids possess dual functionality as promising anticancer agents and advanced NLO materials. Future work should focus on experimental validation, including in vitro enzymatic inhibition assays and spectroscopic evaluation of NLO behavior.

References

Ronca R, Supuran CT. Carbonic anhydrase IX: An atypical target for innovative therapies in cancer. Biochim Biophys Acta Rev Cancer. 2024;1879:189120.

McDonald PC, Chafe SC, Supuran CT, Dedhar S. Cancer therapeutic targeting of hypoxia induced carbonic anhydrase IX: from bench to bedside. Cancers (Basel). 2022;14(14):3297. doi:10.3390/cancers14143297

Aldera AP, Govender D. Carbonic anhydrase IX: a regulator of pH and participant in carcinogenesis. J Clin Pathol. 2021;74(6):350-354.

Rezuchova I, Bartosova M, Belvoncikova P, Takacova M, Zatovicova M, Jelenska L, et al. Carbonic anhydrase IX in tumor tissue and plasma of breast cancer patients: reliable biomarker of hypoxia and prognosis. Int J Mol Sci. 2023;24(5):4325. doi:10.3390/ijms24054325

Chen KT, Seimbille Y. New developments in carbonic anhydrase IX-targeted fluorescence and nuclear imaging agents. Int J Mol Sci. 2022;23(11):6125. doi:10.3390/ijms23116125

Nakashima K, Ichinose T, Watanabe H, Ono M. Comparison of carbonic anhydrase-IX-targeted trifunctional radioligands between linear- and branched-chain arrangements. Front Nucl Med. 2025;5:1585027. doi:10.3389/fnume.2025.1585027

Carbonic anhydrase IX-related tumoral hypoxia predicts worse prognosis in breast cancer: a systematic review and meta-analysis. Front Med (Lausanne). 2023;10:1087270.

Development of benzene and benzothiazole-sulfonamide analogues as selective carbonic anhydrase inhibitors. Bioorg Chem. 2022;128:106060.

Nocentini A, Carta F, Tanc M, Danisman B, Nalbantoglu S, Karatas MO, et al. Synthesis and carbonic anhydrase I, II, VII, and IX inhibition studies with a series of benzo[d]thiazole-5- and 6-sulfonamides. J Enzyme Inhib Med Chem. 2017;32(1):1175-1180.

Nemr MTM, AboulMagd AM, Hassan HM, Hamed AA, Hamed MIA, Elsaadi MT. Design, synthesis and mechanistic study of new benzenesulfonamide derivatives as anticancer and antimicrobial agents via carbonic anhydrase IX inhibition. RSC Adv. 2021;11:26241-26257. doi:10.1039/D1RA05277B

Ureidobenzenesulfonamides as selective carbonic anhydrase I, IX, and XII inhibitors. Molecules. 2023;28(23):7782.

Expanding chemical space of N-acyl sulfonamides for carbonic anhydrase IX inhibitors. Bioorg Chem. 2025;[volume pending]:[pages/article number pending].

Almansour NM. Computational discovery of selective carbonic anhydrase IX (CA IX) inhibitors via pharmacophore modeling and molecular simulations for cancer therapy. Int J Mol Sci. 2025;26(17):8465. doi:10.3390/ijms26178465

Discovery of non-sulfonamide carbonic anhydrase IX inhibitors through structure-based virtual screening. Phys Chem Chem Phys. 2024;26(11):8767-8774. doi:10.1039/D3CP05846H

Entrance-channel plugging by natural sulfonamide antibiotics in carbonic anhydrase IX. Chem Biol Drug Des. 2025;[volume pending]:[pages/article number pending].

Inhibitor binding to metal-substituted metalloenzyme: sulfonamide binding in CA IX. Trends Anal Chem. 2024;[volume pending]:[pages/article number pending].
Aayishamma I, Purawarga Matada GS, Pal R, Ghara A, Aishwarya NVS, Kumaraswamy B, et al. Benzothiazole a privileged scaffold for cutting-edges anticancer agents: exploring drug design, structure-activity relationship, and docking studies. Eur J Med Chem. 2024;279:116831. doi:10.1016/j.ejmech.2024.116831
Benzothiazole derivatives in the design of antitumor agents. Arch Pharm (Weinheim). 2024;[volume pending]:e2400259. doi:10.1002/ardp.202400259
Synthesis and biological evaluation of novel benzothiazole derivatives. Front Chem. 2024;12:[article number pending].
Novel 2-substituted benzothiazole derivatives as possible anticancer drugs. RSC Adv. 2025;[volume pending]:[pages/article number pending].
Design, synthesis and anticancer evaluation of sulphonamido-benzothiazole derivatives. Arab J Chem. 2025;18(11):[article number pending].
Crafting optical wonders: the interplay of electron push-pull dynamics and π-conjugation in nonlinear optics. New J Chem. 2025;[volume pending]:[pages/article number pending].
Dynamic effects on the nonlinear optical properties of donor-acceptor systems. Mater Today Commun. 2025;[volume pending]:[article number pending].
Roadmap for designing donor-π-acceptor fluorophores in UV-Vis and NIR regions: synthesis, optical properties and applications. Biomolecules. 2025;15(1):119. doi:10.3390/biom15010119
Neese F. Software update: the ORCA program system-Version 5.0. WIREs Comput Mol Sci. 2022;12(5):e1606. doi:10.1002/wcms.1606
ORCA. ORCA quantum chemistry program package [Internet]. FACCTs GmbH; [cited 2026 Mar 13]. Available from: https://www.faccts.de/orca/
Lu T, Chen F. Multiwfn: a multifunctional wavefunction analyzer. J Comput Chem. 2012;33(5):580-592. doi:10.1002/jcc.22885
Avogadro Chemistry. Avogadro: an advanced molecular editor and visualization platform [Internet]. [cited 2026 Mar 13]. Available from: https://avogadro.cc/
Eberhardt J, Santos-Martins D, Tillack AF, Forli S. AutoDock Vina 1.2.0: new docking methods, expanded force field, and Python bindings. J Chem Inf Model. 2021;61(8):3891-3898. doi:10.1021/acs.jcim.1c00203
Daina A, Michielin O, Zoete V. SwissADME: a free web tool to evaluate pharmacokinetics, drug-likeness and medicinal chemistry friendliness of small molecules. Sci Rep. 2017;7:42717. doi:10.1038/srep42717
Pires DEV, Blundell TL, Ascher DB. pkCSM: predicting small-molecule pharmacokinetic and toxicity properties using graph-based signatures. J Med Chem. 2015;58(9):4066-4072. doi:10.1021/acs.jmedchem.5b00104